Magnetic behaviour of nickel-cyclam complexes in mesoporous silica: EPR investigations

2009 J. Phys.: Condens. Matter 21 076004

(http://iopscience.iop.org/0953-8984/21/7/076004)

J. Phys.: Condens. Matter **21** (2009) 076004 (9pp) doi:10.1088/0953-8984/21/7/076004

Magnetic behaviour of nickel-cyclam complexes in mesoporous silica: EPR investigations

L Laskowski[1,2,3], A Kassiba[1,2,5], M Makowska-Janusik[3], A Mehdi[4], A Gibaud[1,2], N Errien[1,2] and J Swiatek[3]

[1] Laboratoire de Physique de l'Etat Condensé LPEC, UMR CNRS no 6087, Université du Maine Avenue Olivier Messiaen 72085, Le Mans CEDEX 9, France
[2] Institut de Recherche en Ingénierie Moléculaire et Matériaux Fonctionnels IRIM2F, FR CNRS no 2575, France
[3] Institute of Physics, Jan Dluogosz University, Aleja Armii Krajowej 13/15, 42-200 Czestochowa, Poland
[4] Institut Charles Gerhardt, UMR 5253 Chimie Moléculaire et Organisation du Solide, CC 1701 Université Montpellier II Place E. Bataillon, F-34095 Montpellier Cedex 5, France

E-mail: kassiba@univ-lemans.fr

Received 1 September 2008, in final form 16 October 2008
Published 29 January 2009
Online at stacks.iop.org/JPhysCM/21/076004

Abstract
Electron paramagnetic resonance (EPR) investigations are carried out on mesoporous silica (SBA15) functionalized by Ni-cyclam complexes (1,4,8,11-tetraazacyclotetradecane groups chelating nickel ions). The magnetic behaviour of nickel-cyclam groups, their mutual interactions and dispersions in the mesoporous silica are compared with respect to the doping rates and the synthesis procedures. The spin–spin interactions and the relaxation processes were clarified from the thermal evolution in the temperature range (4 K, 300 K) of the paramagnetic spin susceptibilities and EPR line widths. Thus, the relaxation mechanisms seem marked by the Jahn–Teller effect on the nickel ions mediated by exchange interactions between nearest spins. Isolated Ni-cyclam molecules are involved in some samples while others show the formation of clusters where phonon-assisted one-dimensional (1D) ferromagnetic ordering occurs below 45 K. The performed experiments point out the efficiency of the EPR technique to probe the degree of functionalization of mesoporous silica by Ni-cyclam molecules and to give valuable feedback to improve the synthesis routes.

(Some figures in this article are in colour only in the electronic version)

1. Introduction

Mesoporous materials have attractive architectures over a wide range of functionalization by active molecular groups or nanoparticles for use in potential applications [1–3]. Several strategies for the synthesis routes have been developed to obtain the well known SBA-15 mesoporous silica with variable pore size ranging from 2 to 50 nm. This is the main requirement for selective functionalization of the pores by suitable active groups [4–6]. Also, nanoparticles or functional molecules for magnetic, optical and charge transfer properties can be grafted onto the channels or even incorporated in the silica backbones (see for instance [7, 8]). The high specific surfaces ensure the grafting of a large number of active groups required for catalysis [9, 10], biosensing [11], drug delivery [12, 13] or other molecular engineering [14]. However, the main problem encountered in the functionalization process lies in the formation of aggregates or clusters of the active groups. A sensitive method to probe the degree of agglomeration or dispersion is then required to monitor the yield and achievement of the synthesis process. The original approach considered below concerns paramagnetic organometallic molecules used as functional vectors in mesoporous silica. The EPR

[5] Author to whom any correspondence should be addressed.

technique allows easy probing of these active species including their local environment, dispersion in the host matrix and the correct achievement of the functionalization. In this context, the present work deals with EPR investigations of SBA-15 mesoporous silica functionalized by cyclam moieties (1,4,8,11-tetraazacyclotetradecane) chelating nickel ions (Ni-cyclam). Two synthesis procedures have been developed and the performed investigations are devoted to probe the valence states and the magnetic properties of the nickel based organometallic groups. The EPR spectral parameters (line widths, intensities, g-factors and hyperfine structures) are investigated in the temperature range (4 K, 300 K) and compared for samples obtained by two synthesis procedures. Depending on the synthesis method used, the EPR spectra show an exchange narrowing in some samples or a drastic broadening and low magnetic field shift of the resonance positions for others. These relaxation effects correlate with the organization of the Ni-cyclam groups in clusters where magnetic interactions hold and can even show cooperative magnetic phenomena at low temperatures. As a matter of fact, both isolated Ni-cyclam groups and clusters coexist in the investigated samples with different ratios depending on the synthesis procedure. The paramagnetic spin susceptibilities and the relaxation phenomena evolution versus the temperature, point out the relevant dynamic Jahn–Teller effect on the nickel ions mediated by exchange interactions [15]. A magnetic ordering at low temperature (∼45 K) is clearly demonstrated when only clusters prevail in the samples. Based on an analogy with EPR reports in magnetic materials or in samples with charge transfer properties [16–19], we propose suitable organizations of Ni-cyclam groups inside clusters leading to ferromagnetic ordering in selective samples while in others, the agglomerations did not exhibit any defined magnetic order even at 5 K.

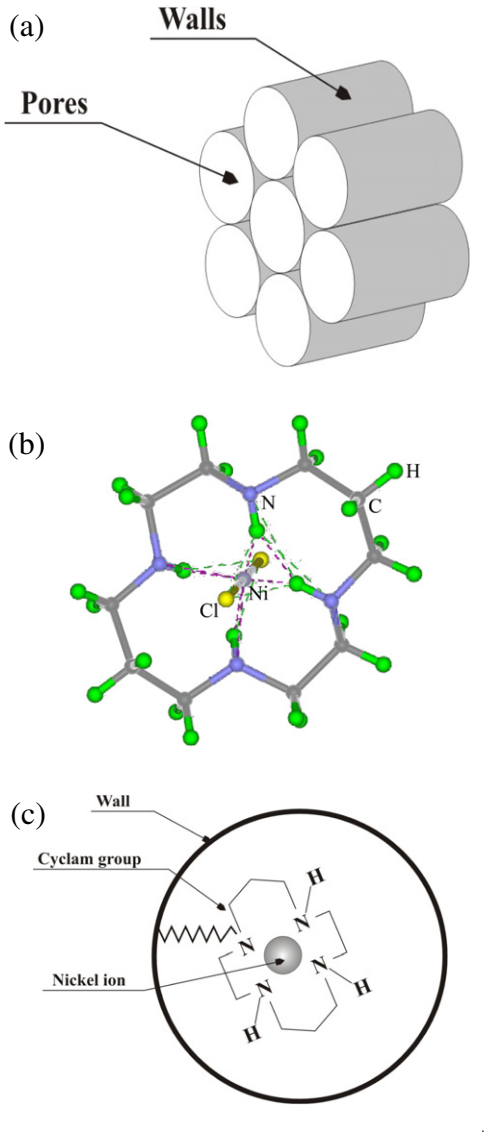

Figure 1. Structure and functionalization of mesoporous silica: (a) mesoporous silica with a hexagonal lattice, (b) structure of Ni-cyclam molecule, (c) a schematic representation of one mesoporous silica pore functionalized by a Ni-cyclam group.

2. Experimental details

2.1. Materials

Two families of mesoporous powders functionalized by nickel-cyclam molecules were synthesized according to the process described in [8, 20]. The samples possess strictly the same structure (figure 1), but they differ in the procedure used to graft the nickel-cyclam molecules inside the mesopores and also in the nickel complex doping ratios. Two procedures (A or B) were performed, as exhaustively described in [20]. The expected differences lie in the dispersion of active groups (Ni-cyclam) in the host matrices and then different magnetic behaviours of the nickel based molecules. The investigated samples are hereafter referenced as (SA5) from procedure (A) and (SB2, SB5, SB11) from procedure B. The doping rates by Ni-cyclam are (2%) in sample SB2, 5% in samples SA5, SB5 and 11% in SB11.

Detailed investigations of the samples (SA5, SB2,5,11) focusing on their composition and morphology as well as their vibrational and optical properties are reported in [20]. The forthcoming EPR investigations focus mainly on electronic, magnetic and paramagnetic properties of Ni-cyclam groups with regard to the doping ratios and the synthesis procedures.

2.2. EPR experimental details

EPR measurements were conducted on a Bruker EMX spectrometer equipped by continuous-wave (CW) X-band (9.5 GHz). The EPR spectra were recorded with microwave powers in the range 20–200 mW and by using a magnetic field modulation of about 5 G. All experimental parameters are chosen to avoid any saturation or distortion of the EPR spectra and to allow an exhaustive comparison between the investigated samples. EPR measurements at variable temperatures (4–300 K) are performed by using an Oxford Instruments cryostat with a precision of about ±0.1 K. For the calibration of the g-factors, a dried DPPH sample characterized by ($g_{\mathrm{DPPH}} = 2.0036$) was used. The EPR spectra simulation

and the evaluation of the EPR spectral parameters (magnetic $\tilde{g}$ and hyperfine $\tilde{A}$ tensor components) were carried out by using commercial Bruker software (Winsimfonia, X-Sophe). The features of the EPR signal are reproduced by using derivative of Lorentzian functions. In this case, the intensity of the EPR signal corresponds to its integrated intensity.

3. EPR results and analysis

3.1. Procedure (A): SA5 sample

3.1.1. General features of EPR spectra. CW-EPR spectroscopy is used to characterize the effective achievement of the sample synthesis and its correct functionalization by the active groups. Figure 2 reports the thermal evolution of EPR spectra recorded on the SA5 sample in the given temperature range (200 K, 5 K). A single EPR line is clearly shown below 200 K and its intensity increases when the temperature is varied from 200 to 60 K. Additionally, a net narrowing of the line width is observed down to 60 K. At lower temperatures, the intensity loss and the development of broad features are indicative of magnetic ordering which will be discussed below.

3.1.2. Identification of the paramagnetic centres. The EPR signal of nickel ions in sample SA5, consists of a single and symmetric line located at the effective g-factor $= 2.20(3)$ at 100 K. This value corresponds to nickel ions in the valence state Ni^{3+}, with an effective spin $S = 1/2$ and electronic configuration ^2E_g as a ground state. The absence of anisotropy, hyperfine or superhyperfine couplings with nearest ligands such as chlorine or nitrogen ions, suggests the formation of Ni-cyclam clusters in the SA5 sample. Following the concentration or the degree of agglomeration of paramagnetic species in the host matrix, the spin–spin interactions contribute to the EPR line shape and width according to two main processes. In the one hand, spin–spin dipolar interaction contributes to the EPR line broadening which can be important depending on the distance and concentration of interacting spins. On the other hand, spin–spin exchange interactions are involved when the distance between spins is too small to allow overlapping of the atomic orbital related to the paramagnetic ions (Ni^{3+}). In this case, the EPR line width undergoes an exchange narrowing with strength depending on the magnitude of the coupling between interacting spins.

In the SA sample, the EPR spectra seem marked by the spin–spin exchange interactions between Ni^{3+} with regard to the exchange narrowed and structureless EPR line. Also, an exhaustive analysis of the relaxation mechanisms and the involved interactions is carried out based on the thermal evolution of the EPR signal features.

3.1.3. Thermal behaviour of the EPR spectra

EPR line intensity. When the temperature is varied from 200 to 5 K, the EPR line intensity increases first, saturates around 60 K and undergoes a drastic decrease below 45 K. This behaviour is commonly observed in spin systems where cooperative magnetic interactions are involved as in dense magnetic materials. The relevance of this statement is supported by the shape of the EPR spectra in the high temperature regime ($T > 60$ K) being exchange narrowed without any detail from anisotropy effects or from some coupling with ligands. Within a simple scheme of interacting nickel based molecules, an adjustment of the thermal behaviour of the EPR line intensity was achieved by using the Curie–Weiss law $\chi(T) = \frac{C}{T-\theta}$ (figure 3(a)). The parameter ($\theta = 38$ K) indicates that ferromagnetic exchange interactions hold between spins which can also be represented by a magnetic exchange integral (J) through the relation:

$$\frac{J}{K_B} = -\frac{3\theta}{2zS(S+1)} \approx -38 \text{ K}$$

$S = 1/2$ refers to the Ni^{3+} ion and z represents the number of interacting ions.

Below 60 K, the departure of the experimental intensity from the Curie–Weiss law and the rapid decrease of the EPR line intensity is a consequence of cooperative magnetic interactions in agreement with the drastic broadening of the

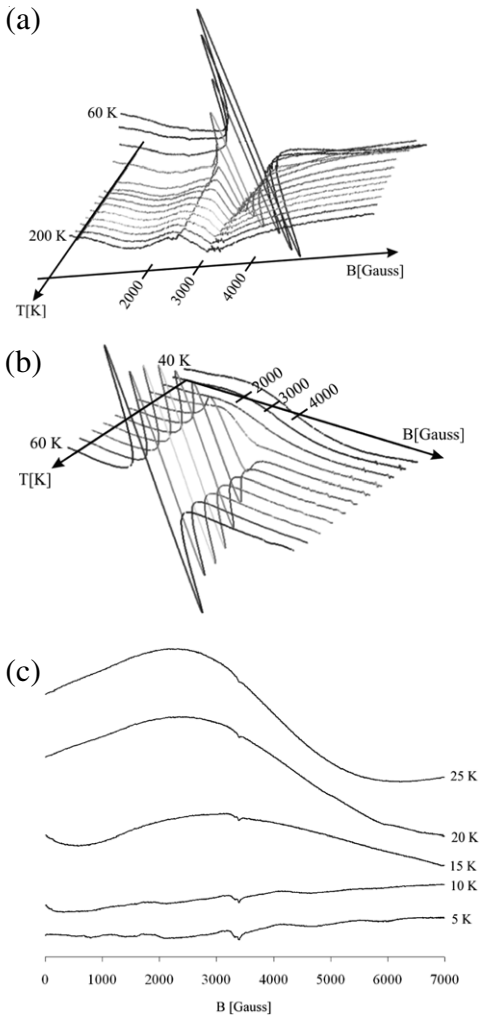

Figure 2. Thermal evolution of EPR spectra of mesoporous silica functionalized by 5.3% Ni-cyclam inside channels (sample SA5) in the temperature ranges 200–60 K (a), 60–40 K (b) and 25–5 K (c).

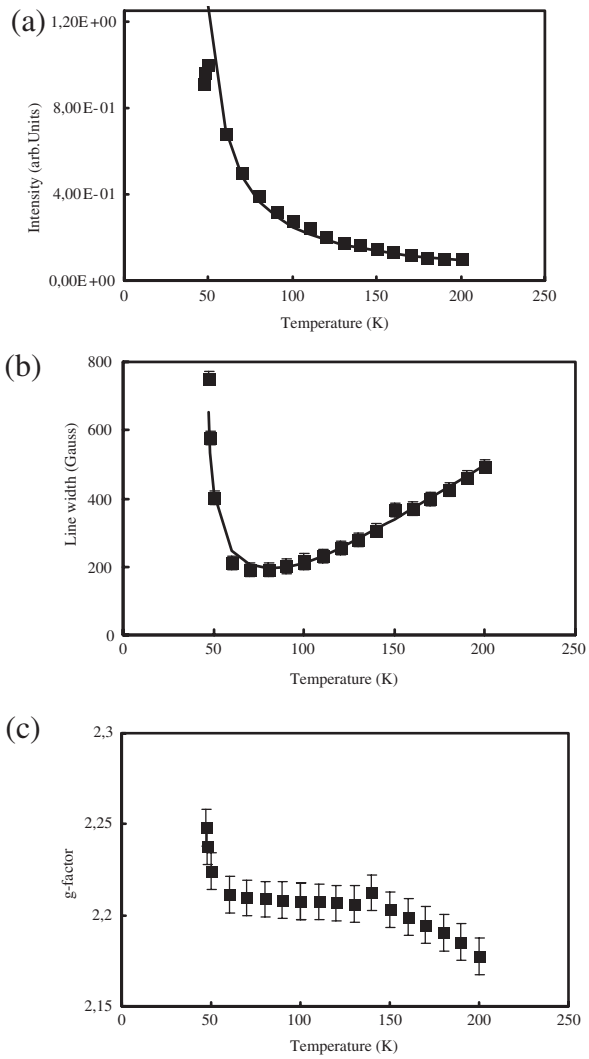

Figure 3. Thermal evolutions of the EPR spectra features: integrated intensity (a), line width (b) and g-factor (c) in sample SA5. The continuous line on the EPR line intensity represents the Curie–Weiss law while the one in (b) represents the relaxation law according to the model discussed in the text.

line width discussed below. Thus, clusters of Ni-cyclam groups seem to be formed in the sample, giving rise to the observed cooperative magnetic phenomena at low temperatures in a similar way to that expected in dense magnetic media.

EPR line width. In the temperature range (200 K, 60 K), a monotonous decrease of the line width (ΔH) with the temperature is observed and can be interpreted either by a linear or an exponential variation law due to the not so extended temperature range. In analogy with former EPR reports on systems with ferromagnetic or anti-ferromagnetic interactions resulting from spin–spin exchange coupling [18] or due to charge transfer in cluster [19], the line width was accounted for by using the following contributions:

$$\Delta H(T) = \Delta H(0) + bT + B\exp(-\tilde{\Delta}/k_{\mathrm{B}}T). \qquad (1)$$

In this equation, $\Delta H(0)$ represents a background line width which accounts for the intrinsic finite EPR line width as well as an eventual spread of the g-factor due to inhomogeneous environments around the spin probes. The second term (b) can be induced by a relaxation which results from pair formation [21] in agreement with the possible existence of clusters, as suggested from the EPR line intensity analysis. The third term (B) is related to a relaxation mechanism from phonon-controlled tunnelling processes [19, 21] with the ($\tilde{\Delta}$) parameter being the energy of an excited vibronic state. This contribution is induced by the dynamic Jahn–Teller effect where the tunnelling between the involved configurations of the Ni-cyclam groups is a phonon-assisted process. However, a similar temperature dependent term can also results from the so-called Orbach–Aminov relaxation, as exhaustively discussed in [21]. This process occurs from a mixing between electronic and nuclear wavefunctions via an excited vibronic state of energy $\tilde{\Delta}$. The distinction between the two processes depends on the magnitude of parameter (B) introduced in equation (1). For instance, in samples with Cu^{2+} ions [21], the phonon-controlled tunnelling is characterized by parameter (B) of the order of the tunnelling frequency (10^6–10^7 s^{-1}) between the Cu^{2+} Jahn–Teller configurations, while for the Orbach–Aminov relaxation process, (B) is of the order of (10^{12}–10^{13} s^{-1}). But, in all processes, the vibronic energy ($\tilde{\Delta}$) in this case is expected to be in the range 100–300 cm^{-1} [21]. However, other authors claim that when the relaxation implies higher excited vibronic states, higher values of $\tilde{\Delta}$ can be obtained as discussed in [19].

In addition to the considered contributions in (equation (1), the divergence of the line width at low temperature suggests the manifestation of a magnetic phase transition [16]. Indeed, in a magnetic material or when clusters of paramagnetic species are involved, spin–spin exchange interactions support the occurrence of a magnetic transition. In this case, the magnetic ordering, ferromagnetic or anti-ferromagnetic, is involved in the Ni-cyclam based clusters and induces a divergence of the correlation length of spin–spin interactions at the critical temperature ($T_{\mathrm{c}} \approx 45$ K). The relaxation mechanism due to the magnetic ordering contributes to the line width by a divergent term as $\Delta H_{m.o} = (T - T_{\mathrm{c}})^{-\nu}$ where the critical exponent ν depends on the dimensionality of the interactions [22] and characterizes the correlation length of magnetic interactions in clusters. Based, on these phenomena, an adjustment of the line width versus the temperature is achieved by using the equation (1) and by considering the above critical contribution. The fitting curve of the EPR line width requires only two main terms; i.e. the critical contribution due to a magnetic ordering and the one from the dynamic Jahn–Teller effect mediated by the spin–spin exchange interaction according to the following expression:

$$\Delta H(T) = A(T - T_{\mathrm{c}})^{-\nu} + B\exp(-\tilde{\Delta}/k_{\mathrm{B}}T).$$

The obtained fitting parameters are

$$A\ (\mathrm{G}\cdot\mathrm{K}^{0.5}) = 920, \qquad T_{\mathrm{c}} = 45\ \mathrm{K}, \qquad \nu = 0.5,$$

$$B\ (\mathrm{G}) = 2040 \qquad \text{and} \qquad \left(\frac{\tilde{\Delta}}{K_{\mathrm{B}}}\right) = 315\ \mathrm{K}.$$

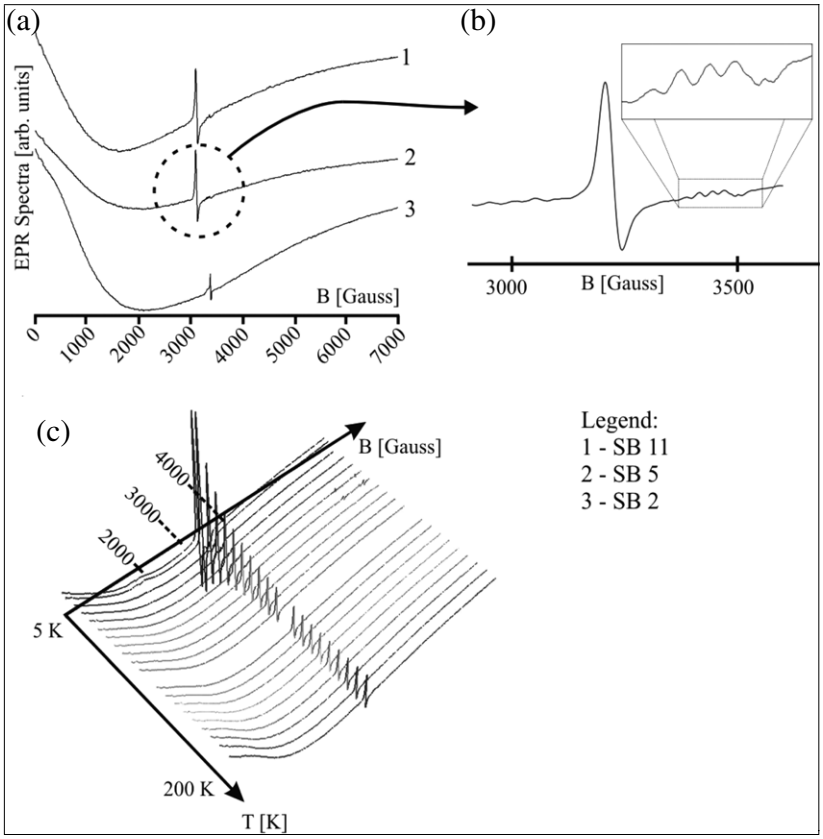

Figure 4. (a) EPR spectra recorded at 100 K for the Ni-cyclam groups incorporated in mesoporous silica (samples SB2,5,11). (b) EPR spectrum recorded at 100 K on sample SB5 with a magnification of a superhyperfine structure and (c) EPR spectra of sample SB5 versus the temperature.

The energy barrier $\tilde{\Delta}$, of the order of 220 cm^{-1}, makes us confident in the correct assignment of the relaxation process as monitored by the Jahn–Teller effect on the Ni^{3+} ions. However, the amplitude $B \sim 10^{10}$ s^{-1} cannot discriminate clearly between the phonon-controlled tunnelling or the Orbach–Aminov relaxation phenomena.

Thus, the thermal variation of the line width seems to be marked by two main regimes. The high temperature behaviour is related to a relaxation mechanism driven by the dynamic Jahn–Teller effect mediated by spin–spin exchange interactions. The low temperature behaviour exhibits the features encountered at a magnetic phase transition. In this case, a drastic line broadening and line position shift are induced by internal magnetic fields which develop between neighbouring magnetic sites (Ni-cyclam). The fitted critical parameter $\nu = 0.5$ is relevant for a system with one-dimensional ferromagnetic interactions due to the negative exchange parameter deduced from the EPR line intensity evolution with temperature [22]. Based on these considerations, a qualitative organization of the Ni-cyclam groups in sample SA5 is proposed and discussed in section 4.

Effective g-factor. The variation of the line position versus the temperature is similar to the line width evolution and seems to bring the mark of cooperative magnetic interactions involved in clusters. When the temperature approaches the critical value (45 K), an increase of the effective g-factor is observed. The g-factor variation depends on the strength of the exchange interaction parameters, as was discussed in [23] where spin probes are surrounded by magnetic ions of the host media. In the case of Ni-cyclam groups, nickel pair formation or a dense magnetic environment around the spin probes contributes to the line position shifts. The critical behaviour around 45 K is consecutive to the cooperative magnetic phenomena. This leads to local magnetic fields around the spin probes and contributes to shifts of the corresponding EPR line features.

Thus, as a summary of the EPR investigations of sample SA5, it is worth noting the relevance of cluster formations in the sample obtained by synthesis procedure (A). The relaxation mechanisms are monitored by the dynamic Jahn–Teller effect at high temperature mediated by the exchange interactions between Ni^{3+} ions. Cooperative phenomena are involved and lead to a magnetic transition below 45 K with the features of ferromagnetic-like order. The behaviour of the EPR spectrum at lower temperatures ($T < 25$ K) is mainly marked by a rapid decrease of the intensity accompanied by a drastic broadening and line position shifts similar to the situation involved in dense magnetic materials.

3.2. Synthesis procedure (B): SB2,5,11 samples

3.2.1. General features of EPR spectra. The EPR spectra recorded at 100 K are summarized in figure 4 for samples SB2,5,11 functionalized in the pores by different doping rates

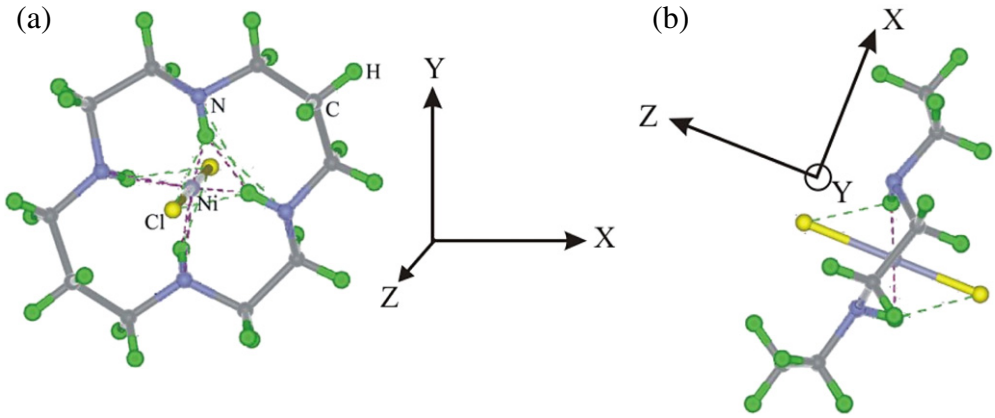

Figure 5. Ni-cyclam molecule bonded to two chlorine ions, the axes X, Y are in the plane of the molecule (a) while the axis Z is along the bond Cl–Ni–Cl (b).

of Ni-cyclam groups. At a first glance, the doping ratio is directly traduced on the central and well resolved EPR signal around $g = 2.18$. The existence of a superhyperfine structure on the EPR spectra indicates the dispersion of the nickel based groups inside the silica pore. However, the broad absorption background observed in the low magnetic field range is a consequence of the formation of agglomerated groups. To perform a quantitative comparison with the carried out experiments on sample SA5, we limit the following analysis of EPR signals to sample SB5 doped, as sample SA5, with 5.3% Ni-cyclam molecules.

3.2.2. Assignment of the paramagnetic centres in sample SB5. Excluding the broad resonance features observed at low magnetic field (figure 4(a)) due to agglomerated species, the central part of the spectra consists in well resolved structure with a magnification shown in figure 4(b). The EPR signal features correlate with superhyperfine couplings with the chlorine ions located in the vicinity of Ni^{3+} ions, in agreement with the structural analysis carried out by Raman and ultraviolet–visible (UV–vis) absorption [20]. However, it is worth noting that the absence of superhyperfine coupling (SHC) between nickel and nitrogen ions of the cyclam rings remains an unresolved problem. The only possibility can be found through weak SHC parameters, i.e. very low compared to the EPR line width.

The simulation of the EPR spectra is quite well traduced by using the powder-like spectrum with the following spin Hamiltonian:

$$H = \beta \vec{B} \cdot \tilde{g} \cdot \vec{S} + \sum_i \vec{S} \cdot \tilde{A}_i \cdot \vec{I}_i,$$

where $\vec{B}$ represents the magnetic field, $\tilde{g}$ the effective magnetic tensor, $\vec{S}$ the electronic spin operator of Ni^{3+} ($S = 1/2$) and $\tilde{A}_i$ the superhyperfine tensor with chlorine ions (nuclear spin $\vec{I}_i = 3/2$ for the main abundant isotope). Adjustments of the EPR spectra were performed by using commercial software from Bruker (X-Sophe). The EPR parameters used to reproduce correctly the experimental spectra are determined in the magnetic frame Ni-XYZ depicted in figure 5. In the fitting procedure, we have considered two configurations of

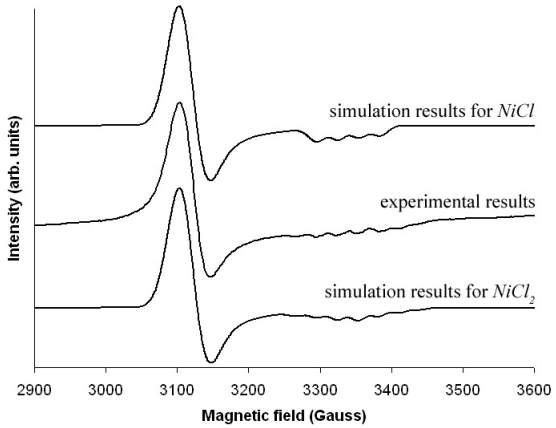

Figure 6. Experimental EPR spectrum of sample SB5 and simulated spectra taking into account a bonding of Ni-cyclam with one chlorine or two chlorine ions.

Ni-cyclam which differ by the number of bonded chlorine ions. The best fit (figure 6) is realized when two chlorine ions are bonded to nickel according to the configuration drawn in figure 5. The EPR parameters used for the simulation are reported in table 1. These results show that the coordination of a nickel-cyclam molecule to two chlorine ions (figure 5) is the main configuration involved in the investigated materials, in agreement with the UV–vis absorption and Raman experiments reported elsewhere [20].

Thus, in contrast to sample SA5, more distributed Ni-cyclam molecules are indeed involved in the SB5 sample. These isolated groups give rise to resolved details of the superhyperfine interactions between Ni^{3+} and the surrounding chlorine ions. The forthcoming analysis is devoted to the thermal behaviour of EPR spectra related to such isolated molecules. The main goal is to discriminate between phenomena involved as a consequence of interactions between active groups or due to the intrinsic Ni-cyclam conformational or electronic changes with the sample temperature.

3.2.3. Thermal behaviour of EPR spectra. As was conducted on sample SA5, a comparative thermal evolution of the EPR

Table 1. EPR parameters (g-tensor, hyperfine coupling and line width) for isolated Ni-cyclam molecules in sample SB5 with the referential frame defined in figure 5.

gx	gy	gz	Ax (G)	Ay (G)	Az (G)	$\Delta H_{X,Y}$ (G)	ΔH_Z (G)
2.178	2.178	2.0025	0	0	28	23	11

spectra was carried out in the temperature range (4 K, 300 K) (figure 4(c)). The thermal evolution is monotonous without any noticed singularities as was reported for sample SA5.

The line intensity versus the temperature is shown in figure 7 where the solid line represents a law ($I(T) = D + \frac{C}{T}$) which testifies to the relevance of isolated spins and the involvement of a Pauli contribution (D). The ratio between the Pauli-like and Curie-like parameters ($C/D \approx 100$) testifies to the possibility of weak charge transfer on the nickel environments. Note, however, that there are no spin–spin exchange interactions leading to some cooperative phenomena as was shown in sample SA5. This is also supported by the line width behaviour of the SB5 EPR spectra which consists in a very weak amplitude variation in the range (30 G, 40 G) compared to (200 G, 800 G) in sample SA5. The slight monotonous increase of line width when the temperature is varied from 300 to 4 K is thought to underline the gradual breakdown of motional averaging at the nickel sites with regard to freezing of torsional and vibrational local modes of the cyclam groups. Thus, no cooperative Jahn–Teller effect seems to manifest itself on such isolated Ni-cyclam molecules involved in sample SB5.

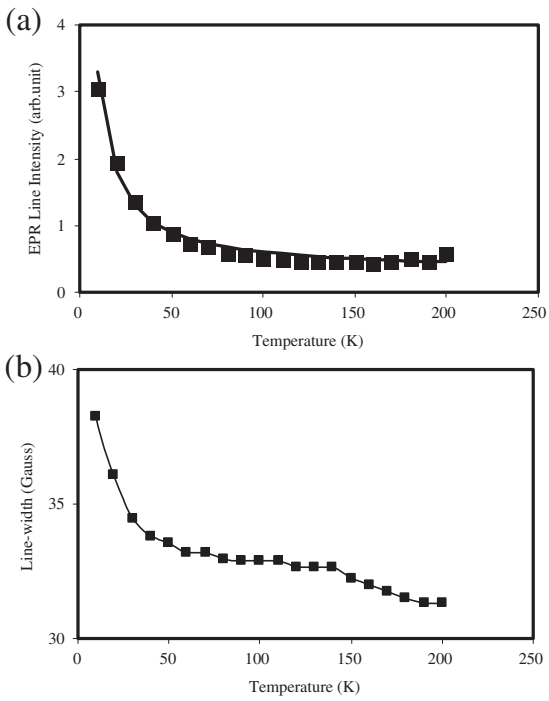

Figure 7. EPR spectrum intensity (a) and a tendency curve as a Curie law (solid line) with small Pauli-like and Curie-like contributions and the line width of the main central line (b) versus the temperature in sample SB5.

4. Discussion

The EPR investigations in sample SA5 point out a moderate spin–spin exchange interaction mediating Jahn–Teller interaction at high temperatures ($T > T_c$) and leading to the cooperative character of the magnetic interactions below T_c. The magnetic ordering below T_c is ferromagnetic-like with regard to the exchange interaction energy term ($J < 0$) deduced from the Curie–Weiss temperature. This magnetic ordering holds in SA5 due to the nickel based molecules being arranged in clusters instead of being regularly dispersed as in the SB5 sample. The main criteria which support our interpretation in sample SA5 can be summarized as follows.

- The exchange narrowed features of the EPR signal in the high temperature regime is consistent with the Curie–Weiss law leading to exchange interaction parameters of about -38 K, i.e. of the order of values involved in one-dimensional Heisenberg ferromagnet inorganic systems [23] or organometallic ones [24].
- The thermal evolution of the EPR line intensity with a maximum at around 60 K is consistent with cooperative magnetic interactions in the clusters marked at low temperature ($T < 45$ K) by a very broad signal with the features of EPR spectra in dense magnetic material or when magnetic ordering is established.
- The line width divergence at a critical temperature of 45 K is a consequence of the divergence of correlation lengths characteristic of magnetic domain scales or clusters of Ni-cyclam molecules.
- The critical line width contribution $\Delta H(T) \propto A(T - T_c)^{-\nu}$ with the exponent $\nu = 0.5$ indicates the occurrence of magnetic interaction along one defined direction (1D-like system) [22, 25]. However, as magnetic order cannot occur in a pure 1D-like system, we should consider the contribution of the electron–phonon interaction which is thought to originate from the Jahn–Teller effect on the nickel ions mediated by the ferromagnetic interactions between Ni-cyclam groups.

In contrast, the isolated Ni-cyclam groups involved in the SB5 sample did not show any singular behaviour or magnetic interactions. The only relaxation mechanism which seems to monitor the EPR line width correlates with the motional (torsion, vibration) averaging at the nickel sites. However, in addition to isolated Ni-cyclam centres, agglomerations of Ni-cyclam groups are also present in the SB5 sample, as identified by the low magnetic field EPR signal. These broad features did not show any critical variation with the temperature and even their intensity decreases at low temperatures, in agreement with dense magnetic domains without any defined order.

The EPR results, obtained on selective synthesis batches, can be schematically traduced by the Ni-cyclam arrangements expected to hold in the SA5 and SB5 samples (figure 8);

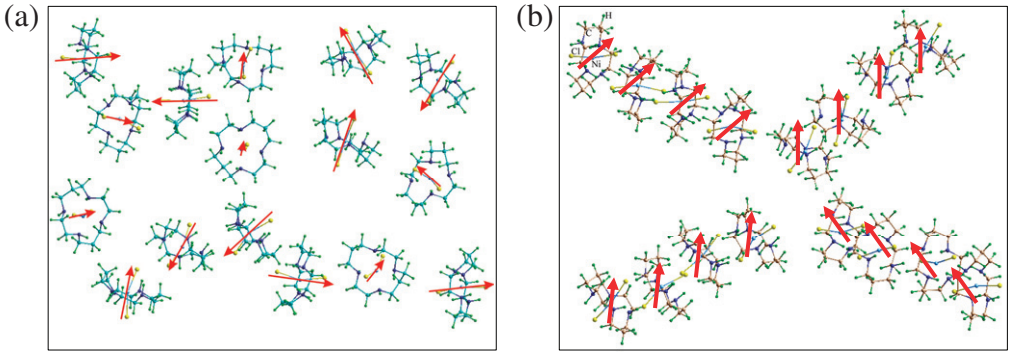

Figure 8. Agglomerated Ni-cyclam groups without defined magnetic order (a) as involved in sample SB5 and linear fragments of Ni-cyclam molecules with ferromagnetic coupling between nearest moments (b) expected to hold in sample SA5. The arrows depict the magnetic moments located on nickel ions.

the isolated Ni-cyclam groups in sample SB5 are not considered. The schema (figure 8(a)) illustrates agglomerated and disordered Ni-cyclam molecules. This configuration gives rise to the broad EPR signal at the low magnetic field side and no particular magnetic ordering is established even at low temperature. In contrast, the Ni-cyclam clusters of figure 8(b) are arranged as linear fragments with schematically ferromagnetic-like order. This schema accounts for EPR measurements below 45 K where ferromagnetic coupling between nearest spins along each linear fragment is involved with respect to the scaling parameter ($\nu = 0.5$). It is worth noting that the configurations reported in figure 8 did not take into account the silica matrices. The agglomerations in sample SB5 can be segregated inside the pores while in SA5 samples we cannot exclude the possibility of 1D Ni-cyclam islands being grafted in different regions of the silica walls. This is a possible requirement to support the 1D-magnetic ordering realized in the SA5 sample below 45 K.

5. Conclusion

Exhaustive EPR investigations and analyses are carried out on mesoporous silica functionalized by Ni-cyclam molecules. The EPR signals from isolated paramagnetic centres or arranged in clusters are identified and assigned judiciously. The EPR data clarify the effective location of nickel in the cyclam groups, their dispersion in the host silica matrices for one synthesis batch (B) and the ferromagnetic exchange interactions between nearest spins in the (A) batch. Indeed, in sample SA5, magnetic interactions are involved and induce, at the level of clusters, a ferromagnetic ordering at low temperature (<45 K). The degree of functionalization of the silica by the active groups can be determined from EPR experiments through the observations of isolated molecules, as shown in the SB samples. Based on EPR results, schematic organizations of the Ni-cyclam molecules in the host mesoporous matrices were proposed depending on the synthesis procedure. As a main finding from the studies carried out, we point out the relevance of the EPR spectroscopy to probe the degree of functionalization of mesoporous silica by paramagnetic Ni-cyclam molecules.

Acknowledgments

Part of this work was carried out under bilateral cooperation programme France–Poland-PHC–Polonium 2008.

References

[1] Conçalves M C and Attard G S 2003 *Rev. Adv. Mater. Sci.* **4** 147
[2] Lu Y F, Yang Y, Sellinger A, Lu M C, Huang J M, Fan H Y, Haddad R, Lopez G and Brinker C J 2001 *Nature* **410** 913
[3] Attard G S, Glyde J C and Goltner C G 1995 *Nature* **378** 366
[4] Zhao D, Feng J, Huo Q, Melosh N, Fredrickson G H, Chmelka B F and Stucky G D 1998 *Science* **279** 548
[5] Ryoo R, Ko C H, Kruk M, Antchshuk V and Jaroniec M 2000 *J. Phys. Chem.* B **104** 11465
[6] Corriu R, Mehdi A and Reyé C 2004 *J. Organomet. Chem.* **680** 4437
[7] Anwander R 2001 *Chem. Mater.* **13** 4419
[8] Corriu R 2003 *J. Organomet. Chem.* **686** 32
[9] Consul J M D, Peralta C A, Benvenutti E V, Riuz J A C, Pastore H O and Baibich I M 2006 *J. Mol. Catal.* A **246** 33
[10] Taguchi A and Schüth F 2005 *Micropor. Mesopor. Mater.* **77** 1
[11] Slowing I, Trewyn B G, Giri S and Lin V S Y 2007 *Adv. Funct. Mater.* **17** 1225
[12] Tang Q, Xu Y, Wu D and Sun Y 2006 *Chem. Lett.* **35** 474
[13] Ji X, Hu Q, Hampsey J E, Qiu X Q, Gao L, He J and Lu Y 2006 *Chem. Mater.* **18** 2265
[14] Jal P K, Patel S and Mishra B K 2004 *Talanta* **62** 1005
[15] Li M M, Zou L J and Zheng Q Q 1998 *J. Appl. Phys.* **83** 6596
Kassiba A, Makowska-Janusik M, Alauzun A, Kafrouni W, Mehdi A, Reyé C, Corriu R J and Gibaud A 2006 *J. Phys. Chem. Solids* **67** 875
[16] Rettori C *et al* 1997 *Phys. Rev.* B **55** 3083
[17] Kassiba A, Hrabanski R, Bonhomme D and Hader A 1995 *J. Phys.: Condens. Matter* **7** 3339
[18] Pud A A, Tabellout M, Kassiba A, Korzhenko A A, Rogalsky S P, Shapoval G S, Houze F, Schneegans O and Emery J R 2001 *J. Mater. Sci.* **36** 3355
Zhechera E, Stoyanova R, Alcantara R, Lavela P and Tirado J L 2002 *Pure. Appl. Chem.* **74** 1885
[19] De D K 1986 *Phys. Rev.* B **34** 4651
[20] Laskowski L, Errien N, Makowska-Janusik M, Kassiba A, Kodjikian S, Alauzun J, Mehdi A, Swiatek J and Gibaud A 2009 in preparation
[21] Hoffmann S K, Hilczer W, Gosiar J, Massa M M and Calvo R 2001 *J. Magn. Reson.* **153** 92

[22] Goni A, Lezame L, Espina A, Trobajo C, Gracia J R and Rojo T 2001 *J. Mater. Chem.* **11** 2315
[23] Misra S K and Kahrizi M 1983 *Phys. Rev.* B **28** 5300
Sichelschmidt J, Loidl A, Baenitz M, Geibel G, Steglich F and Otto H H 2000 arXiv:cond-mat/0005346 v1
[24] Green M L H, Harrison A, Mountford P and Ng D K P 1993 *J. Chem. Soc. Dalton Trans.* **14** 2215
[25] Richards P M 1976 *Proprieta Locali alle Tarnsizioni di Fase* ed K A Muller and A Rigamonti (Amsterdam: North-Holland)